Fano resonance and magneto-optical Kerr rotaion in periodic Co/Ni complex plasmonic nanostructure*

Le-Yi Chen(陈乐易), Zhi-Xiong Tang(唐志雄), Jin-Long Gao(高锦龙), Dao-Yong Li(李道勇), Cheng-Xin Lei(类成新), Zhen-Zhi Cheng(程振之), Shao-Long Tang(唐少龙)†, and You-Wei Du(都有为)

Collaborative Innovation Center of Advanced Microstructures, Nanjing National Laboratory of Microstructures, Jiangsu Key Laboratory for Nanotechnology and Department of Physics, Nanjing University, Nanjing 210093, *China*

(Received 30 May 2016; revised manuscript received 13 August 2016; published online 30 September 2016)

We report a pure ferromagnetic metallic magnetoplasmonic structure consisting of two-dimensional ordered Ni nanodisks array on Co film. With a sufficient height of the nanodisks, a steep and asymmetric Fano resonance can be excited in this structure. We attribute the fascinating spectral lineshape to the strong coupling between the excitation of surface plasmon polaritons at the interface and the localized surface plasmon resonance of nanodisks. The conclusion is fully confirmed by spectrum measurements in nanostructures with different heights. Furthermore, the enhancement and sign of the magneto-optical Kerr rotation in this structure are significantly modified by the Fano resonance.

Keywords: magneto-optics, surface plasmons, magnetoplasmonics, magneto-optical devices

PACS: 33.57.+c, 73.20.Mf, 78.20.Ls, 85.70.Sq **DOI:** 10.1088/1674-1056/25/11/113301

1. Introduction

Benefited from the development of plasmonics, we can concentrate the light in sub-wavelength scale to break the diffraction limit and manipulate it more delicately and efficiently via the excitation of the surface plasmons (SPs).[1–3] Such fascinating modification of the electromagnetic field leads to lots of nonlinear optical effects,[4,5] and it even results in magneto-optical (MO) effects in non-magnetic nanocomposites.[6] Therein, the magnetoplasmonics combining magneto-optics and plasmonics has attracted extra attention due to the multifunctionality that can enhance the MO effects and control SPs actively.[7–9] This leads to a variety of applications, such as ultra-sensitive detector,[10,11] optical isolators,[12,13] ultra-precise MO ruler,[14] etc. The demonstration of the SPs and the consequent enhancement of the MO effects have been well discussed in magnetoplasmonic nanostructures.[15–18] However, there is a non-negligible problem in most of nanocomposites. The incorporation of non-FM materials would dilute the volume fraction of ferromagnetic (FM) materials, which accordingly weakens the overall MO effect, though the effect has been enhanced due to the excitation of SPs.[19]

A direct pathway to overcome this problem is to fabricate magnetoplasmonic structures using pure ferromagnetic (FM) metals. However, due to the Ohmic losses, the typical FM metals cannot provide a sharp SP resonance which usually brings a significant enhancement of the MO effect.[9,20] The Fano resonance possessing a steep, asymmetric line shape is considered as a proper alternative to be implanted into the pure FM magnetoplasmonic structures.

The underlying mechanism of Fano resonance is accepted as the coupling between a narrow discrete resonance and an overlapping broad one.[21] It can be caused by the interference between surface plasmon polariton (SPP) modes,[22] between localized surface plasmon (LSP) modes of different parts,[23] or between the LSP mode and the Rayleigh anomalies.[24] In this work, we introduce a new type of Fano resonance, resulting from the coupling between overlapped LSP and SPP modes in the pure FM magnetoplasmonics structure, by constructing two-dimensional (2D) ordered Ni nanodisks on Co film. Two samples with different heights of the Ni nanodisks are prepared to reveal the origin of the Fano resonance and the influence to the MO Kerr rotation.

2. Sample fabrication

Our samples were fabricated mainly by magnetron sputtering, interference lithography (IL), and electrochemical deposition. A layer of Co film was deposited on a clean 2×2 cm^2 silicon wafer with the thickness of 50 nm by magnetron sputtering. A 150-nm-thick photoresist (Allresist, ARP-3170) was spin-coated on the prepared Co substrate. After a pre-bake at 95 °C for 1 min, the photoresist was exposed by a home-made Lloyd's mirror system. The diameter of the laser beam of a 442-nm-wavelength He–Cd laser was pre-expanded to 8.0 cm to construct large-area highly ordered nanostructures. The substrate was exposed twice separately along the two orthogonal directions. After immersed in a developing solution for 45 s (Allresist, AR 26), a square lattice pattern of holes was

*Project supported by the National Key Project of Fundamental Research of China (Grant No. 2012CB932304) and the National Natural Science Foundation of China (Grant Nos. 11374146 and U1232210).

†Corresponding author. E-mail: tangsl@nju.edu.cn

© 2016 Chinese Physical Society and IOP Publishing Ltd

produced. O_2 plasma etching was used to remove the residual resist inside the holes to facilitate the following electrochemical deposition. Ni was electrodeposited into the ordered array of holes from a solution containing 15 g/L $NiSO_4 \cdot 6H_2O$ and 30 g/L H_3BO_3 with the current density of 0.1 mA/cm^2. After the final remove process of dipping samples into acetone in a 60 °C water bath for 10 min, the ordered Ni nanodisks were constructed on the Co film. According to the principle of interference lithography, the period of the pattern can be given by $\lambda/(2\sin\theta)$, where λ is the laser wavelength and θ is the incident angle of the laser beam. The height of the Ni nanodisks depends on the time of the electrochemical deposition. Here, we fabricated samples with two different kinds of heights, named A for the 50-nm-high one and B for the 125-nm-high one.

Figure 1(a) shows the top view of the Co/Ni complex plasmonic nanostructure by scanning electron microscope. It is clearly seen that the magnetoplasmonic structure containing Co film and 2D ordered Ni nanodisks without obvious defects being obtained. The diameter of the nanodisks is about 200 nm and period of the 2D array is about 380 nm. Figure 1(b) shows the 3D model of the Co/Ni complex plasmonic nanostructure, and a rectangular coordinate system has been built. The relative orientation between the incident light and the sample is described by the incident angle θ and the azimuthal angle φ, which are both shown in Fig. 1(b).

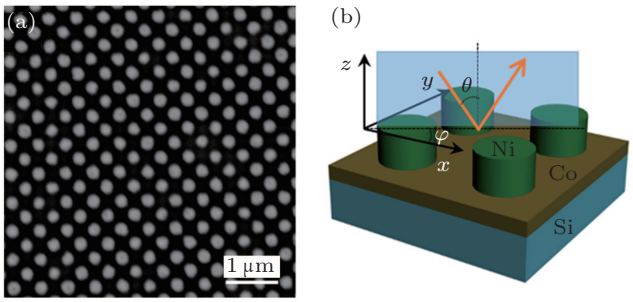


Fig. 1. (color online) Topography of the Co/Ni complex plasmonic nanostructure. (a) Scanning electron micrograph of the Co/Ni complex plasmonic nanostructure. The diameter of the nanodisks is approximately 200 nm. The period is 380 nm. (b) 3D model of the Co/Ni complex plasmonic nanostructure.

3. Simulation results

Unlike the noble metals, Ni provides a relatively flat LSP resonance due to the intrinsic large damping.[9] The extinction cross sections of the 200-nm-radial Ni nanodisks with 50 nm height and 125 nm height were calculated by the FDTD method, as shown in Fig. 2(a). The extinction spectra show the characteristic peak of the excitation of the LSP mode.[25] It is seen that both of the two LSP resonances span over more than 200 nm in the spectral range in Fig. 2(a), and the central positions are near 680 nm without any obvious shift with the change of the height. Thus, the LSP mode in the Ni nanodisk is not appropriate to provide the narrow resonance to form Fano resonance, while it can play the role of the broad one.

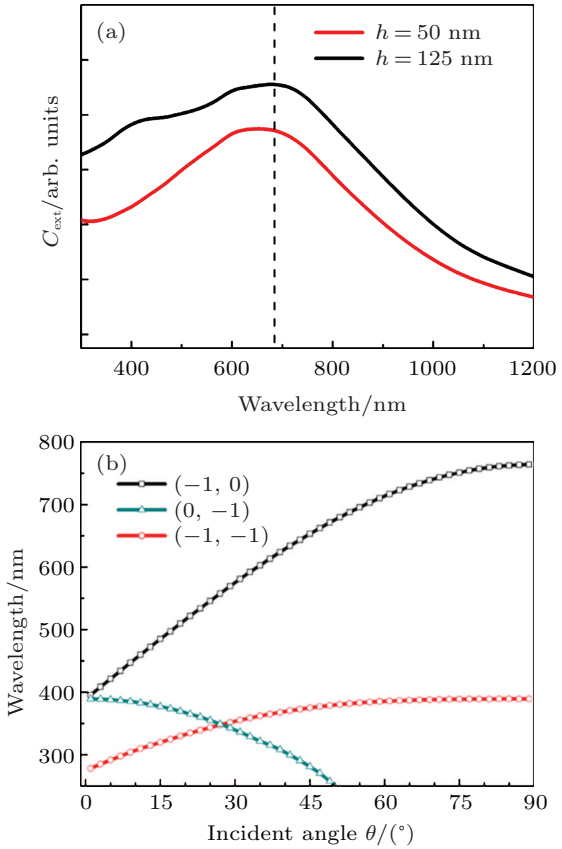


Fig. 2. (color online) Simulated results of LSPs and SPPs. (a) Calculated extinction cross-sections C_{ext} for the single Ni nanodisks with 50 and 125 nm heights by the FDTD method. (b) The θ dependence of the calculated incident wavelengths to excite SPP modes for several diffraction orders according to the momentum match condition at the period of 380 nm.

Besides the LSP resonance from the single Ni nanodisk, the ordered array can excite SPP modes at the interface by grating coupling. The momentum match condition can be used to obtain the relation between the wavelength of the incident light and the incident angle for the given diffraction orders and the certain period, which can be expressed as[26]

$$k_{spp}(\lambda) = \frac{2\pi}{\lambda}\sqrt{\frac{\varepsilon_d\varepsilon_m}{\varepsilon_d+\varepsilon_m}}, \tag{1}$$

$$\mathrm{Re}(k_{spp}(\lambda)) = \left| ik_0\sin\theta\cos\varphi + jk_0\sin\theta\sin\varphi + im\frac{2\pi}{d} + jn\frac{2\pi}{d}\right|, \tag{2}$$

where λ is the wavelength of incident light and the wavenumber $k_0 = (2\pi/\lambda)\varepsilon_d$ and ε_m are the permittivity of the dielectric and metal. d is the period of the grating, and (m, n) are the 2D diffraction orders of reciprocal lattice vectors. The incident angle θ and the azimuthal angle φ have been defined herein before.

According to the momentum match condition, the incident wavelengths to excite SPP modes for several diffraction orders were calculated, as shown in Fig. 2(b). It can be seen

that the excitation wavelength of the (−1, 0) order SPP mode falls in the overlapped region with the spectral positions of the LSP resonance when the incident angle is near 45°. In this condition, it is reasonable for the (−1, 0) order SPP mode to provide the narrower resonance, coupled with the broad LSP resonance, to obtain the Fano resonance.

4. Experimental results and discussion

The excited SP modes in magnetoplasmonic structures are related to the polarization state of the incident light. For the TE-polarized incident light, whose E field is perpendicular to the incident plane, the electrons in Ni nanodisks are driven along the y axis by the E field with a phase lag ascribed to damping when $\varphi = 0°$, according to the coordinate system in Fig. 1(b). The collective forced oscillator of the free electrons is considered as the physical nature of the LSP.[25] For the TM-polarized incident light, whose E field is in the incident plane and perpendicular to the direction of propagation, the forced oscillator of the free electrons is still existent to excite the LSP mode, but the direction is along the direction of propagation. Besides, the z-component of the E field results in a charge accumulation at the interface. Then the SPP mode can be excited when the momentum match condition is met. Reflected on the spectra, the former shows an absorption peak which has weak dependence on the incident angle, while the latter additionally shows the SPP resonance whose spectral position is determined by the momentum match condition. Especially, when the LSP mode and SPP mode are excited in a similar spectral position, the strong coupling between them possibly leads to a steep, asymmetric Fano-like spectral lineshape.

According to the results of the simulations, the LSP mode of the Ni nanodisks and the (−1, 0) order SPP mode in our samples are excited simultaneously when the TM-polarized light impinges on the interface with the incident angle near 45°. However, for TM-polarized incident light on Sample A, as shown in Fig. 3(a), there is only an ordinary dip at each angle of incidence, instead of Fano-like spectra. The position of the dip shifts from 630 nm to 700 nm as the increase of the incident angle, which agrees well with the calculated (−1, 0) order SPPs in Fig. 2(b). This indicates that the dip corresponds to the resonance of the SPP mode. In Fig. 3(b), no obvious absorptions can be observed for the TE-polarized light, which indicates the absence of LSP mode. This conclusion can also be confirmed by the simulation results in the insets. For TE-polarized light, neither obvious local nor propagating modes exist, while for TM-polarized light, no dipole mode can be observed on the nanodisks but they act together with the Co film as a whole surface that supports propagating modes.

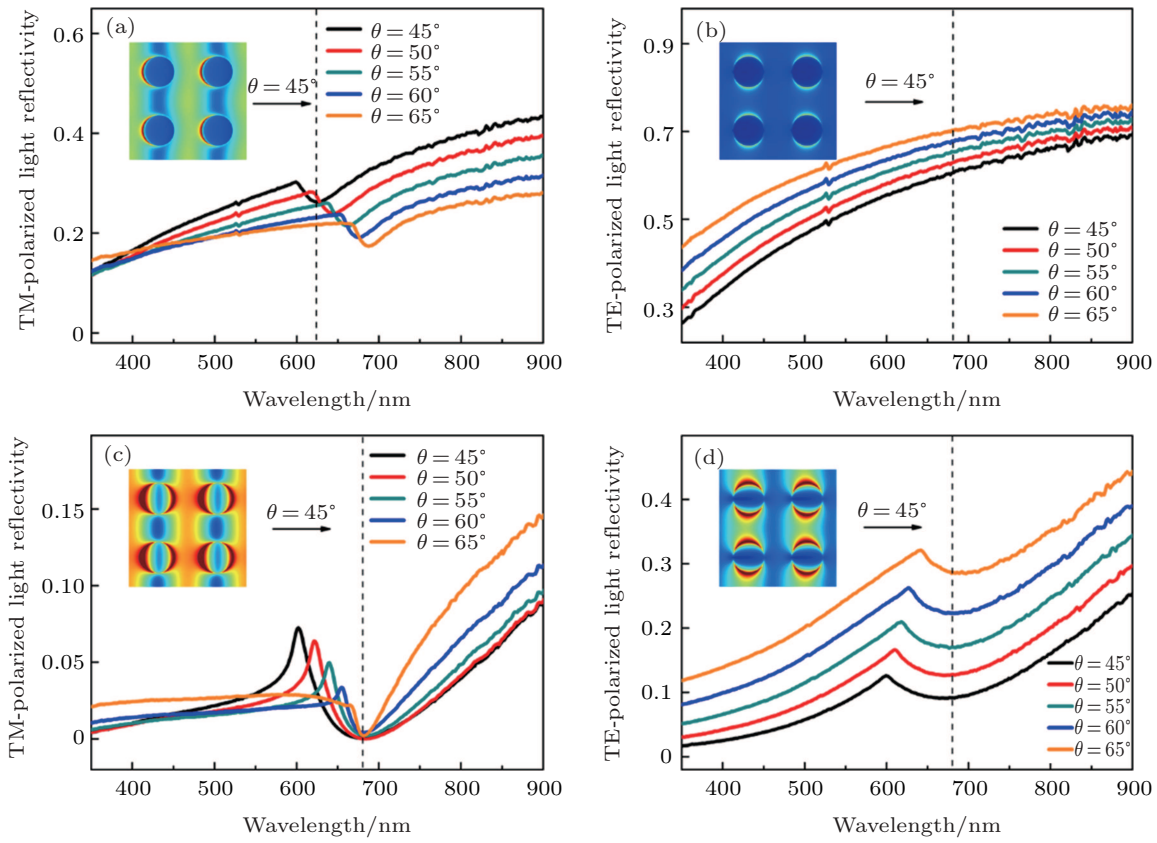


Fig. 3. (color online) Measured reflectivity spectra for $\varphi = 0°$. Insets are the distribution of the E field at the interface. The corresponding incident wavelengths and incident angles are indicated respectively. (a) For Sample A with TM-polarized incident light. (b) For Sample A with TE-polarized incident light. (c) For Sample B with TM-polarized incident light. (d) For Sample B with TE-polarized incident light.

For Sample B, the Fano-like lineshape appears in Fig. 3(c), as we predicted from the results of simulations. In Fig. 3(d), the dips with their central positions at 680 nm can be observed at the incident angle from 45° to 65°, which fits the calculated extinction cross-section in Fig. 2(a). Thus, they are confirmed to be the LSP resonance of the Ni nanodisk, and are visually displayed in the inset. Furthermore, it can been seen in Fig. 3(c) that, the Fano-like spectra lineshape gradually collapses with the increase of the incident angle. The weakening of the LSP mode due to the decrease of the x-component of the E field with the increase of the incident angle is considered to impair the coupling with the SPP mode.

The differences of the reflectivity spectra clearly reveal the difference of inner SP modes between the two samples, which can also be reflected on the longitudinal MO Kerr rotation spectrum in Fig. 4. The longitudinal MO Kerr rotation was measured at $\varphi = 0°$ and $\theta = 45°$ for TM-polarized light with a home-made MOKE measurement system.[26] The magnetic field up to 1.5 kOe was applied in longitudinal configuration using an electromagnet. The weighted summation of the measured results of Co and Ni flat films according to the area fraction in our samples was shown as a reference. The Kerr spectrum of 50-nm-high Sample A almost coincides with the reference curve in most of the spectral range except the enhancement near the position of the SPP resonance. The non-significant enhancement, which can be seen more clearly in the inset, is attributed to the reflectivity reduction due to the excitation of the SPP mode in Fig. 3(a).[9] In sharp contrast to Sample A, the Fano resonance with the steep and asymmetric spectral lineshape brings the obvious enhancement and reversal of the Kerr rotation to Sample B in the whole Fano region. The manipulation of the sign of rotation of the reflected light's polarization is usually considered to be due to the phase adjustment of LSPs, and can be employed to devise new schemes for high-resolution biochemo sensing.[10] Here, the sign change is realized in the Co/Ni complex nanostructure via the generation of the Fano resonance.

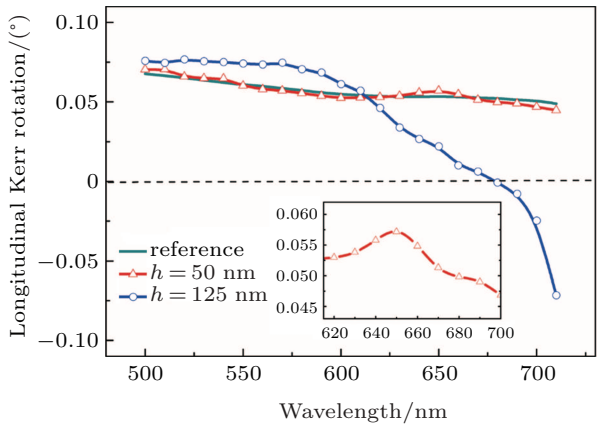


Fig. 4. (color online) Measured longitudinal MO Kerr rotation for TM-polarized light at $\varphi = 0°$ and $\theta = 45°$. The inset is the measured results of Sample A in the spectral range from 615 nm to 700 nm.

The 30-nm-high nanodisk placed on the glass substrate has been reported to excite the LSP resonance on it.[25] However, we cannot find the LSP mode which should appear in Sample A. The LSP mode in nanodisks is considered as the result of the radial spatial confinement.[25] In the Co/Ni complex system where the Ni disks are constructed on the Co film, the collective oscillation of the free electrons on the nanodisks induced by the incident light will rapidly transfer to the conductive Co film, losing the spatial confinement, if the height of the disk is not sufficient, which hinders the excitation of effective LSPs and consequently prevents the Fano resonance.

In our previous work on Co antidots film and Co double layer film, the interaction between different orders' SPPs leads to variety of line shapes of the Kerr spectrum and the enhancement of the MO signal.[26,27] Especially, in Co double layer film, it has been proposed as a possible explanation that an unusual sign change of the Kerr angles is due to the interaction between SPPs from bottom layer and LSPs from top layer.[26] In Sample B, the sign change is observed again. By the comparison between Sample A and B, it is clear that it is the Fano resonance which results in the sign change and the existence of the LSP mode, and Fano resonance is closely linked with the heights of the Ni disks.

5. Conclusions

In conclusion, we have fabricated the Co/Ni complex nanostructure, with 2D ordered Ni nanodisks on Co film, by the interference lithography and electrochemical deposition. The longitudinal MO Kerr spectrum is significantly modified by the Fano resonance, not only the enhancement but also the reversal of the rotation. Thus, it can be a promising way to produce coupled plasmonic devices in macroscopic scale, acting as a new type of MO-based ultrahigh sensitive biochemical sensors.[10,11] By comparison between the two samples with different heights of the ordered Ni nanodisks, it can be seen that the strong coupling between the LSP mode and the SPP mode is the fundamental source of the Fano resonance in our Co/Ni complex nanostructure. Either the lack of any SP mode or the imbalance of their intensity will destroy the Fano-like spectral lineshape.

References

[1] Heber J 2009 *Nature* **461** 720
[2] Polman A 2008 *Science* **322** 868
[3] Najafov H, Lee B, Zhou Q, Feldman L C and Podzorov V 2010 *Nat. Mater.* **9** 938
[4] Kneipp K 2007 *Physics Today* **60** 40
[5] Wurtz G A, Pollard R and Zayats A V 2006 *Phys. Rev. Lett.* **97** 057402
[6] Gu Y and Kornev K G 2010 *J. Opt. Soc. Am. B* **27** 2165
[7] Armelles G, Cebollada A, García-Martín A, García-Martín J M, González M U, González-Díaz J B, Ferreiro-Vila E and Torrado J F 2009 *J. Opt. A* **11** 114023
[8] Temnov V V, Armelles G, Woggon U, Guzatov D, Cebollada A, García-Martín A, García-Martín J M, Thomay T, Leitenstorfer A and Bratschitsch R 2010 *Nat. Photon.* **4** 107

[9] Armelles G, Cebollada A, García-Martín A and González M U 2013 *Adv. Opt. Mater.* **1** 10
[10] Bonanni V, Bonetti S, Pakizeh T, Pirzadeh Z, Chen J, Nogués J, Vavassori P, Hillenbrand R, Åkerman J and Dmitriev A 2011 *Nano Lett.* **11** 5333
[11] Maccaferri N, Gregorczyk K E, de Oliveira T V, Kataja M, van Dijken S, Pirzadeh Z, Dmitriev A, Åkerman J, Knez M and Vavassori P 2015 *Nat. Commun.* **6** 6150
[12] Chin J Y, Steinle T, Wehlus T, Dregely D, Weiss T, Belotelov V I, Stritzker B and Giessen H 2013 *Nat. Commun.* **4** 1599
[13] Belotelov V I, Kreilkamp L E, Akimov I A, Kalish A N, Bykov D A, Kasture S, Yallapragada V J, Gopal A V, Grishin A M, Khartsev S I, Nur-E-Alam M, Vasiliev M, Doskolovich L L, Yakovlev D R, Alameh K, Zvezdin A K and Bayer M 2013 *Nat. Commun.* **4** 2128
[14] Zubritskaya I, Lodewijks K, Maccaferri N, Mekonnen A, Dumas R K, Åkerman J, Vavassori P and Dmitriev A 2015 *Nano Lett.* **15** 3204
[15] Banthí J C, Meneses-Rodríguez D, García F, González M U, García-Martín A, Cebollada A and Armelles G 2012 *Adv. Mater.* **24** Op36
[16] Krutyanskiy V L, Kolmychek I A, Gan'shina E A, Murzina T V, Evans P, Pollard R, Stashkevich A A, Wurtz G A and Zayats A V 2013 *Phys. Rev. B* **87** 035116
[17] González-Díaz J B, García-Martín A, Armelles G, García-Martín J M, Clavero C, Cebollada A, Lukaszew R A, Skuza J R, Kumah D P and Clarke R 2007 *Phys. Rev. B* **76** 153402
[18] Ferreiro-Vila E, González-Díaz J B, Fermento R, González M U, García-Martín A, García-Martín J M, Cebollada A, Armelles G, Meneses-Rodríguez D and Sandoval E M 2009 *Phys. Rev. B* **80** 125132
[19] González-Díaz J B, García-Martín A, Armelles G, Navas D, Vázquez M, Nielsch K, Wehrspohn R B and Gösele U 2007 *Adv. Mater.* **19** 2643
[20] Johnson P B and Christy R W 1974 *Phys. Rev. B* **9** 5056
[21] Luk'yanchuk B, Zheludev N I, Maier S A, Halas N J, Nordlander P, Giessen H and Chong C T 2010 *Nat. Mater.* **9** 707
[22] Belotelov V I, Akimov I A, Pohl M, Kotov V A, Kasture S, Vengurlekar A S, Gopal A V, Yakovlev D R, Zvezdin A K and Bayer M 2011 *Nat. Nanotech.* **6** 370
[23] Armelles G, Cebollada A, García-Martín A, González M U, García F, Meneses-Rodríguez D, de Sousa N and Froufe-Pérez L S 2013 *Opt. Express* **21** 27356
[24] Kataja M, Hakala T K, Julku A, Huttunen M J, van Dijken S and Törmä P 2015 *Nat. Commun.* **6** 7072
[25] Maccaferri N, Berger A, Bonetti S, Bonanni V, Kataja M, Qin Q H, van Dijken S, Pirzadeh Z, Dmitriev A, Nogués J, Åkerman J and Vavassori P 2013 *Phys. Rev. Lett.* **111** 167401
[26] Xia W B, Gao J L, Zhang S Y, Chen L Y, Tang Y M, Tang S L and Du Y W 2014 *Chin. Phys. B* **23** 103303
[27] Xia W B, Gao J L, Zhang S Y, Luo X J, Chen L Y, Xu L Q, Tang S L and Du Y W 2014 *Opt. Express* **22** 1359